J Inorg Organomet Polym (2017) 27 (Suppl 1):S231–S238
DOI 10.1007/s10904-017-0674-x

A Correlation Study of Subnanoscopic Free Volume and Thermo-physical Properties of Modified Borosilicate Glasses with Progressive Substitution of B_2O_3 by Al_2O_3

Prasanta K. Ojha[1] · Sangram K. Rath[1] · Kathi Sudarshan[2] · Sandeep K. Sharma[2] · Pradeep K. Pujari[2] · Tapas K. Chongdar[1]

Received: 20 April 2017 / Accepted: 7 September 2017 / Published online: 12 September 2017

Abstract The understanding of atomic-scale structure is a prerequisite for establishing the physico–chemical behavior of complex glass systems. To this end, positron annihilation life time spectroscopy (PALS) is an atomic scale probe capable of investigating the subnanoscopic free volume of amorphous materials. In the present work, PALS has been used to quantify the free volume changes as a function of increasing substitution of B_2O_3 by Al_2O_3 in strontium borosilicate glasses intended to be used as sealant in solid oxide fuel cells. The free volume parameters; ortho-positronium (o-Ps) life time (τ_3) and intensity (I_3) show composition dependant variations which are correlated to the molar volume and compactness of the glasses through a commutative free volume parameter, $\tau_3^3 I_3$. The effect of change in nanoscopic free volume induced by the substitution of B_2O_3 by Al_2O_3 on the glass transition temperature (T_g), softening temperature (T_s), coefficient of thermal expansion (CTE) and thermal stability of glasses have been studied. A remarkable trend-based variation in these macroscopic properties with change in free volume is observed. We envisage that the findings of this work will provide new insights in establishing subnanoscopic structure and thermo-physical property correlation of complex glass systems containing multiple network former and modifiers.

✉ Prasanta K. Ojha
prasantaojha@gmail.com; prasanta@nmrl.drdo.in; pkojha77@yahoo.co.in

[1] Naval Materials Research Laboratory, Ambernath, Thane, Maharashtra 421506, India

[2] Radiochemistry Division, Bhabha Atomic Research Centre, Mumbai 400085, India

Keywords Positron annihilation lifetime spectroscopy (PALS) of glass · Free volume of glass · Thermo-physical properties of glass

1 Introduction

Inorganic glasses are technologically important materials which find applications as substrates to optical components, fiber glasses, radioactive waste containment, photochromatic glass, chemically resistant sealing glasses in solid oxide fuel cell (SOFC) and separator among others [1–6]. The oxide glassy materials can be treated as complex, topologically disordered networks with composition specific spatial arrangement of oxide ions. The glass properties are known to depend on such spatial ordering in atomic positions. Adequate understanding of correlation between structure and physical–chemical properties of inorganic glasses is of fundamental interest. Atomic arrangement in glasses is conventionally studied with several techniques like X-ray diffraction [7], neutron diffraction [8–10], infrared (IR) spectroscopy [11], Raman spectroscopy [12, 13], nuclear magnetic resonance (NMR) spectroscopy [14, 15] and extended X-ray absorption fine structure (EXAFS) [16]. However, knowledge of atomic structure per se is not adequate for description of glass structure and physical properties. It is also necessary to probe the atomic-deficient space distribution in the glass matrix, especially at a sub-nanometer scale [17]. The atomic scale free volume available in the glass matrix due to its lack of long range order is a key parameter that governs the physical properties with compositional feature of glasses [11, 18, 19]. Free volume in inorganic glasses is essentially the excess volume in comparison to the thermodynamically equilibrium crystal with same composition [20]. This is a characteristic feature for the structure

of disordered solids due to their metastability. In general, the sources of free volume nano-voids in glass structure are due to electron density distribution of covalent bonds within some atomic configuration [21, 22], fluctuations of structural fragments frozen near glass transition [23] and geometrical inconsistencies between different glass forming structural units [20, 24, 25]. Positron annihilation lifetime spectroscopy (PALS) is one of the most sensitive techniques capable of probing such fine free volume holes and is frequently used to study amorphous polymeric materials [26–29] and glass systems [11, 17, 30].

In general, various components in the glass composition control the local structure and changes in speciation. Such a variation in local ordering greatly affects the thermo-physical properties of SOFC glass sealants. Common network formers like B_2O_3 and SiO_2 are used in SOFC glass sealants which form the basic three dimensional networks in the glass structure and determine the thermal properties like glass transition temperature (T_g), glass softening temperature (T_s), coefficient of thermal expansion (CTE) and adhesion/wetting with other SOFC components. Network modifiers like BaO, SrO, CaO, MgO break the network, create non-bridging oxygen species, maintain charge neutrality and modify glass properties such as T_g, T_s, thermal stability and CTE [31–33].

In the present study a series of strontium aluminoborosilicate glasses were prepared with systematic substitution of B_2O_3 by Al_2O_3 in the glass composition. PALS was used to quantify the composition dependant variation of free volume of glasses through the free volume scaling parameter, $\tau_3^3 I_3$. Thermo-physical properties of the glasses namely glass transition temperature, softening temperature, coefficient of thermal expansion and thermal stability of the glasses were investigated through experimental techniques. Structural parameters like molar volume, compactness, and thermophysical properties of glasses were evaluated vis-à-vis Al^{+3}/B^{3+} ratios in the glass compositions. Structure–property correlations of glasses were established with the free volume as the central structural feature.

2 Experimental

The glasses were prepared by conventional melt quenching method where the batches were melted at 1500 °C and poured onto a brass mould for glass making. The batch composition was designed with formula $45SrO–xAl_2O_3–(45–x)B_2O_3–10SiO_2$ (wt%) with x varying between 0 and 30 wt% at step size of 5 wt%. The batch materials used for glass melting were SiO_2, H_3BO_3, Al_2O_3 and $SrCO_3$. The batch materials were mixed and melted in platinum crucible. The glasses formed upon melt quenching were annealed for 1 h at temperature ~T_g, glass transition temperature, for release of thermal stresses incorporated in the glassy matrix. Each batch was assigned with a code for ease of identification. The code is denoted by abbreviations for each component and a subscript value indicating the wt% of that component. The glasses formed were analyzed for evaluation of properties. In the analyzed glass compositions Al_2O_3 concentration varies from 0 to 26.50 mol% compensating the variation of B_2O_3 from 51.84 to 19.41 mol%. Table 1 includes the batch composition used for preparing the glasses and the code.

The PALS measurement of glass samples were performed at room temperature using plastic scintillation detectors coupled in fast–fast coincidence mode. The time dispersion used for acquisition of PALS spectra was 12.5 ps and the time resolution of the spectrometer was 260 ps (full width at half maximum, measured using ^{60}Co). Each specimen consisted of a system of circular discs, of total size 10 mm diameter and 1.2 mm thickness. A ^{22}Na isotope positron source of 15 μCi activity sealed between two kapton foils (eight μm thick) was sandwiched between two identical sample discs. More than 1×10^6 counts were acquired in each PALS spectrum. In order to estimate the positron annihilation fraction in kapton films as well as in source material, a reference spectrum of Si single crystal was also acquired.

The glass transition temperature, T_g and crystallization temperature, T_p of glass samples were determined by differential scanning calorimetry (DSC) using Setsys 16, SETARAM, France. DSC traces were recorded at heating rate 5 °C/min in the temperature range 25–1200 °C. Thermal stability of glasses was calculated as the temperature lag between glass transition and first crystallization temperature, i.e. ($T_p – T_g$).

Thermal expansion of glass samples was measured using a vertical pushrod type dilatometer of UNITHERM-MTM MODEL 1161 Dilatometer System, Anter Corporatiosn, USA. All measurements were carried out in air. Thermal expansion of glass was measured in temperature range 30–800 °C and at a heating rate of 3 °C/min. Samples used for these measurements were rod shaped with a length of ≈2.5 cm and diameter ≈ 0.5 cm. Linear coefficient

Table 1 Glass composition with code

Glass code	Compositions (mol%)			
	SrO	Al_2O_3	B_2O_3	SiO_2
$Sr_{45}B_{45}S_{10}$	34.82	0.00	51.84	13.34
$Sr_{45}A_5B_{40}S_{10}$	35.47	4.00	46.94	13.59
$Sr_{45}A_{10}B_{35}S_{10}$	36.14	8.16	41.85	13.85
$Sr_{45}A_{15}B_{30}S_{10}$	36.84	12.48	36.56	14.12
$Sr_{45}A_{20}B_{25}S_{10}$	37.56	16.97	31.07	14.40
$Sr_{45}A_{25}B_{20}S_{10}$	38.32	21.64	25.35	14.69
$Sr_{45}A_{30}B_{15}S_{10}$	39.10	26.50	19.41	14.99

of thermal expansion (CTE) α was calculated using the following equation:

$$\alpha = \frac{L_1 - L_0}{L_0 (T_1 - T_0)} = \frac{\Delta L}{L_0 \Delta T} \quad (1)$$

where, L_0 and L_1 are the lengths of the glass specimen at start temperature T_0 under consideration and the end test temperature T_1 respectively. Softening temperature (T_s) of the glass was marked at the temperature of maximum expansion in the expansion plot recorded through dilatometer, following which contraction due to deformation sets in.

3 Results and Discussion

3.1 Subnanoscopic Free Volume Characteristics

The positron lifetime spectra of the glass systems were analyzed using the PATFIT computing program with a three-component model [34]. A preliminary analysis of PALS data after correction for positron annihilations in the source and subtracting the background showed the presence of three lifetime components. The first component was observed to vary in the range of 120–160 ps for different samples. In glassy materials, the short-lived component is usually ascribed to para-positronium (*p*-Ps) annihilation and its intrinsic lifetime being very short is not really affected by the characteristics of the material [30, 35]. The intermediate lifetime (τ_2 ~ 300 ps) is due to annihilation of free positrons with electrons from vacant sites in oxide materials [30]. The longest component varies in the range of 590–650 ps and is ascribed to the ortho-positronium (*o*-Ps) pick-off annihilation in these materials. We attribute the longest lifetime component τ_3 to the pick-off annihilation of *o-Ps* trapped in small intrinsic voids (free volume) present in glass network. Table 2 includes the PALS data recorded for glasses in the investigated series.

The τ_3 can be considered as a measure of the free volume hole size according to Tao-Eldrup model and the pick-off intensity I_3 corresponds to number of these holes present in the glass network [30]. From the data in Table 2 we observe that in the investigated series of glasses, $Sr_{45}B_{45}S_{10}$ (without Al_2O_3) shows the highest τ_3 value and the least I_3 value, while $Sr_{45}A_{30}B_{15}S_{10}$ glass, with the highest Al_2O_3 content, is characterized by lowest τ_3 and highest I_3 values. This implies that the $Sr_{45}B_{45}S_{10}$ is having lesser number but bigger free volume holes, while the $Sr_{45}A_{30}B_{15}S_{10}$, system is characterized by relatively large quantity of smaller holes. However, no systematic variation of either τ_3 or I_3 is observed in the intermediate compositions. The free volume hole radius, R_3 was evaluated from the following correlation between *o*-Ps pick-off lifetime (τ_3) and R_3 [36]:

$$\tau_3 = \frac{1}{2}\left[1 - \frac{R}{R+\Delta R} + \frac{1}{2\pi}\sin\left(\frac{2\pi R}{R+\Delta R}\right)\right]^{-1} \quad (2)$$

The R_3 values obtained from the above equation is presented in Table 2, which also does not show any particular trend w.r.t. the variation in glass composition. On the basis of the data avalaible we are unable to provide any mechanistic insights into the genesis of such variations of the τ_3 and I_3 values with progressive substitution of B_2O_3 by Al_2O_3 in the glass compositions. Hence we use a scaling free volume parameter of $\tau_3^3 I_3$ which can also be considered as a measure of fractional free volume of the glass compositions. In a previous work, we used this scaling parameter to establish the structure–property correlations in a mixed cation borosilicate glass composition as a function of La^{3+}/Sr^{2+} ratios [19].

In this report, the $\tau_3^3 I_3$ values of glass samples are plotted versus the Al^{3+}/B^{3+} ratios in the series of glasses as shown in Fig. 1. In the same plot, variation of molar volume of glasses is also shown for comparison. An initial observation that can be made from Fig. 1 is that the molar volume, a macroscopic property, almost parallels the increasing trend of the nanoscopic free volume parameter with increasing Al^{3+}/B^{3+} ratio in the glass systems. While the free volume parameter $\tau_3^3 I_3$ of the glass system $45SrO–xAl_2O_3–(45–x)B_2O_3–10SiO_2$ increases with increasing 'x' till x = 20 wt% (Al^{3+}/B^{3+} ratio = 0.546) followed by a decrease, the molar volume shows a monotonic increase with increasing Al^{3+}/B^{3+} ratio. It may be

Table 2 PALS data of glass samples

Glass code	PALS data					
	τ_3(ns)	Error	I_3 (AU)	Error	$\tau_3^3 I_3$	R_3 (Å)
$Sr_{45}B_{45}S_{10}$	0.648	0.0220	18.20	2.40	4.952	0.894
$Sr_{45}A_5B_{40}S_{10}$	0.6114	0.0122	23.55	1.58	5.382	0.776
$Sr_{45}A_{10}B_{35}S_{10}$	0.6272	0.0198	21.85	2.70	5.391	0.834
$Sr_{45}A_{15}B_{30}S_{10}$	0.6723	0.0230	18.52	2.35	5.627	0.966
$Sr_{45}A_{20}B_{25}S_{10}$	0.6329	0.0136	24.43	1.89	6.193	0.846
$Sr_{45}A_{25}B_{20}S_{10}$	0.6109	0.0127	26.77	1.93	6.103	0.775
$Sr_{45}A_{30}B_{15}S_{10}$	0.5956	0.0135	28.10	2.31	5.937	0.718

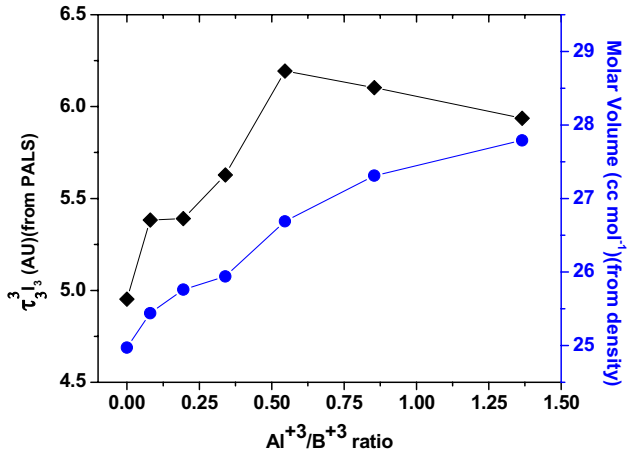

Fig. 1 Variation of free volume and molar volume against Al^{3+}/B^{3+} ratios in the glass composition

noted that there is a discernible change in the rate of increase in the molar volume at an Al^{3+}/B^{3+} ratio of 0.546 marked by the maximum in free volume. The observation of increasing free volume and molar volume of the glass systems suggest the formation of a more open network structure with substitution of B_2O_3 by Al_2O_3 in the glass composition.

Compactness δ of a glass is a measure of the normalized change of the mean atomic volume due to chemical interactions of the elements forming the network of a given solid [37]. Consequently it is more sensitive to changes in the structure of the glass network as compared to the molar volume V_M. The compactness δ was calculated using the equation:

$$\delta = \frac{\sum_i \frac{c_i A_i}{\rho_i} - \sum_i \frac{c_i A_i}{\rho}}{\sum_i \frac{c_i A_i}{\rho}} \quad (3)$$

where c_i, A_i and ρ_i are the atomic fraction, atomic weight and the atomic density of the ith element of the glass and ρ is the measured density of the glass. The error in the density measurement, and consequently in δ was estimated to be less than $\pm 1\%$.

Figure 2 shows variation of the compactness values with Al^{3+}/B^{3+} ratio along with the free volume data as estimated from PALS in order to understand the correlative trend of the structural parameters. From the figure it is evident that with progressive Al_2O_3 substitution of B_2O_3 the compactness of the glasses decreases as a direct consequence of increase in free volume.

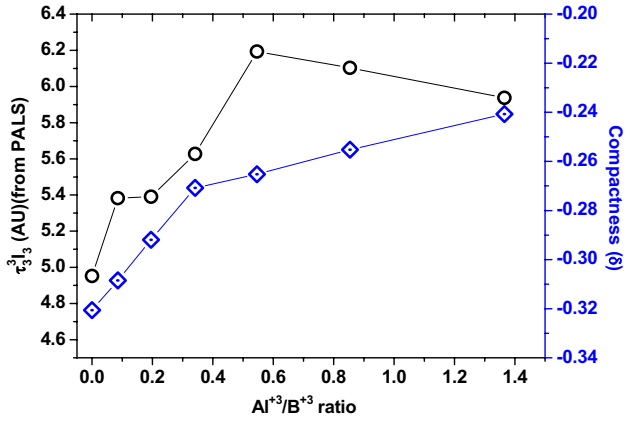

Fig. 2 Variation of free volume and compactness of glass with Al^{3+}/B^{3+} ratios

4 Thermo-physical Properties of Glasses

In the investigated series of glasses, thermo-physical properties like glass transition temperature T_g, crystallization temperature T_p and thermal stability $T_p - T_g$ are determined from the DSC thermogram of samples. Temperature profile of all the glass samples obtained through DSC are superimposed for comparison purpose and shown in Fig. 3. Straight lines shown in the figure are guide to eye for a quick comparison

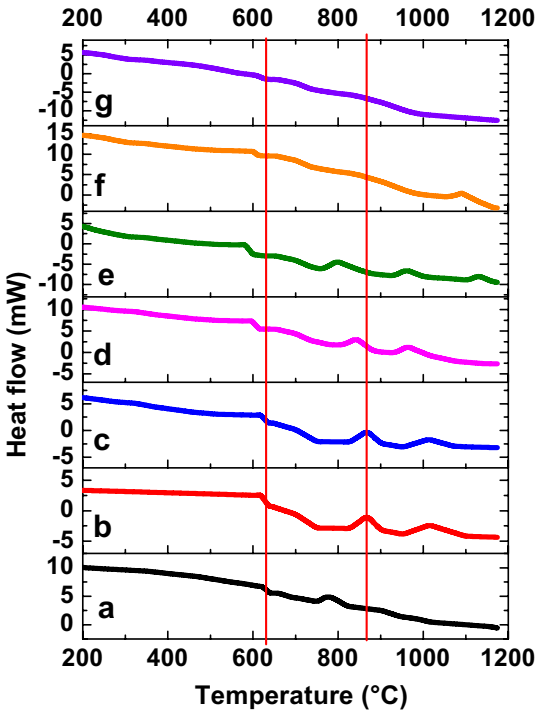

Fig. 3 DSC thermograms of glass samples **a** $Sr_{45}B_{45}S_{10}$, **b** $Sr_{45}A_5B_{40}S_{10}$, **c** $Sr_{45}A_{10}B_{35}S_{10}$, **d** $Sr_{45}A_{15}B_{30}S_{10}$, **e** $Sr_{45}A_{20}B_{25}S_{10}$, **f** $Sr_{45}A_{25}B_{20}S_{10}$, **g** $Sr_{45}A_{30}B_{15}S_{10}$

of characteristic temperatures against compositions. Glass softening temperature T_s and coefficient of thermal expansion CTE are determined experimentally from the thermal expansion data elucidated by dilatometer. Figure 4 includes the plots of thermal expansion of glasses with temperature. A guide line shown in the graph illustrates the variation in T_s with glass composition. Variation of all the characteristic parameters; glass transition temperature T_g, Glass softening temperature T_s, thermal stability $T_p - T_g$ and coefficient of thermal expansion CTE are further correlated with the change in free volume in the glass.

Figure 5 shows the variation of T_g with increase in Al^{3+}/B^{3+} ratio in the glass composition along with the free volume data. The T_g of the glasses decrease with increasing substitution of B^{3+} by Al^{3+} up to Al^{3+}/B^{3+} ratio of 0.546, followed by an increase at higher values.

The most significant observation from Fig. 5 is the remarkable correspondence between the free volume parameter and the T_g. With increase in Al^{3+}/B^{3+} ratios, the free volume content in glasses pass through a maximum while variation in T_g, follows an exactly opposite trend and passes through a minimum. T_g of amorphous materials is the onset of transformation from glassy to a viscoelastic state marked by segmental mobility beyond this temperature. Therefore, free volume content in the glassy matrix is expected to influence the T_g. The decrease in T_g with increasing B_2O_3 substitution by Al_2O_3 in the glass network can be explained by the fact that space requirement for mobility is facilitated by increased free volume and hence less thermal energy required for segmental movements.

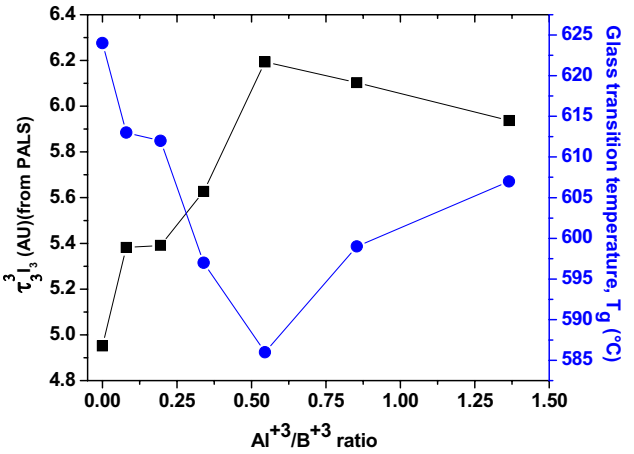

Fig. 5 Variation of free volume and glass transition temperature against Al^{3+}/B^{3+} ratios in glasses

Glass softening temperature T_s, of a glass is determined from the thermal expansion measurement by dilatometer and is ascribed to a temperature where the viscous flow changes to plastic flow, which means the temperature at which the glass may slump under its own weight. In the thermal expansion curve T_s corresponds to the temperature of maximum expansion and beyond which there is a sudden fall in the curve due to piercing of the push rod into the softened glassy matrix. Generally, T_g and T_s though measured by different experimental techniques, both show similar trend with respect to composition and other functional parameters [38–41]. For the investigated series of glasses, a

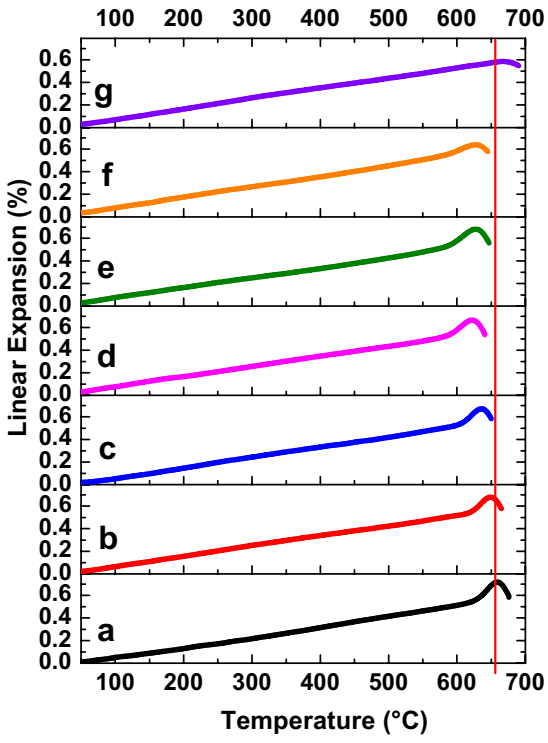

Fig. 4 Thermal Expansion of glasses **a** $Sr_{45}B_{45}S_{10}$, **b** $Sr_{45}A_5B_{40}S_{10}$, **c** $Sr_{45}A_{10}B_{35}S_{10}$, **d** $Sr_{45}A_{15}B_{30}S_{10}$, **e** $Sr_{45}A_{20}B_{25}S_{10}$, **f** $Sr_{45}A_{25}B_{20}S_{10}$, **g** $Sr_{45}A_{30}B_{15}S_{10}$

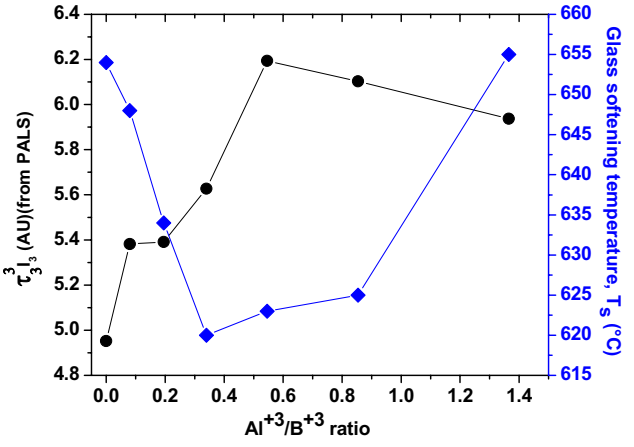

Fig. 6 Variation of free volume and glass softening temperature versus Al^{3+}/B^{3+} ratios in the glasses

plot of variation of T_s is shown against Al^{3+}/B^{3+} ratios in the glass composition and compared with the free volume data of glasses in Fig. 6. The variation of T_s in the investigated series of glasses follows a trend similar to that observed for T_g with increasing Al^{3+}/B^{3+} ratio, the reason being the same as invoked for the relation between T_g and free volume of glasses.

Both T_g and T_s of glasses are important parameters considering the applicability as SOFC sealant. T_g corresponds to a viscosity of $10^{11.3}$ Pa.s and T_s corresponds to a value of $10^{8–9}$ Pa.s [38]. A seal glass is brittle below T_g but viscous above T_g. The stress between the seal glass and the adjoining SOFC components induced by thermal expansion mismatch during thermal cycling may generate cracks, which are potential paths for gas leakage. These cracks can 'self heal' by viscous flow of the seal glass above T_g [42–44]. Therefore at SOFC operational temperature the viscosity of a seal glass should be within 10^5–10^8 Pa.s to provide hermetic sealing. This means hermeticity of a seal glass can be maintained by a T_g value below the SOFC operating temperature while relieving thermal stresses and self-healing cracks. However, T_s of the seal glass should be close to SOFC operating temperature to avoid excessive glass flow under stack load. Above investigation may give an insight to tune the free volume by judicious manipulation of the glass composition so as to maintain the desired T_g and T_s value of the sealing glass.

CTE of the seal glass is considered to be one of the most important thermal properties for its application in SOFCs. During cell operation CTE of seal glass should match with those of other SOFC components to avoid thermal stress. When there is a CTE difference, both tensile (for $CTE_{component} > CTE_{glass}$) and compressive (for $CTE_{component} < CTE_{glass}$) stresses are possible at the interface. To avoid thermal stress CTE difference should be within 1×10^{-6} $°C^{-1}$. Tensile stress often leads to cracks at the interface in the glass. Compressive stress to some extent can be tolerated because the compressive strength of a seal glass is much higher than the tensile strength but excessive compressive stress causes delaminating of the glass from the interfacing SOFC components. In practice, a CTE ranging from 9.0 to 12.0×10^{-6} $°C^{-1}$ is desired for SOFC applications [4]. In the investigated series of glasses, CTE of glasses were calculated from the dilatometer experiment and plotted against Al^{3+}/B^{3+} ratios in the glass composition along with the free volume data in Fig. 7.

A similar trend for both the free volume and CTE of glasses is discernible from Fig. 7; both pass through a maximum at the same Al^{3+}/B^{3+} ratio. In the investigated series of glasses, it is observed that with increasing Al_2O_3 content in the glass matrix as a substitute to B_2O_3 the CTE increases from 10.8 to $11.2 \times 10^{-6} °C^{-1}$ and on further increase CTE decreases to 9.1×10^{-6} $°C^{-1}$. Similar observations of

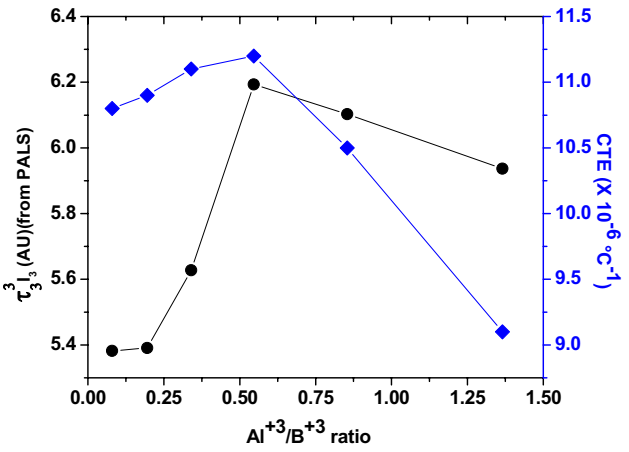

Fig. 7 Plot of variation of free volume and CTE against Al^{3+}/B^{3+} ratios in the glasses

decreasing CTE with increasing Al_2O_3 content have also been observed for other systems [4].

In general, thermal expansion arises due to an increase in average bond length with increasing temperature. The increase in bond length arises from the asymmetry of the potential energy versus inter-atomic distance curve of the Condon–Morse potential energy diagram [39]. In glassy systems, CTE depends on the glass structure symmetry, bond-bending, and molar-free volume. A decrease in glass structure symmetry increases CTE, decreasing bond bending increases CTE and increase in free volume increases CTE [38]. A similar scenario is observed in the present case with both the CTE and free volume following a similar trend.

The thermal stability of the glasses are quantified against their hindrance to crystallization and calculated by $T_p - T_g$, where T_p is the first crystallization temperature. Crystallization is an unwanted process in a seal glass as it affects the thermo-physical and thermo-chemical stability of the glass in operational conditions. Though thermal stability is one of the most critical requirements of SOFC seal glasses, devitrification of multi component glasses still remain an unresolved issue. Phase separation or microheterogenity in the glass structure enhance crystallization. Any thermodynamic parameter which favours the kinetics leads to devitrification in glasses. In all the investigated glasses crystallization temperature could not be noticed in the temperature range 25–1200 °C in the thermographs recorded by DSC. However, in all those glasses where crystallization behavior was observed in DSC, the thermal stability was calculated and is plotted against glass composition and free volume in Fig. 8.

From the figure it is observed that the thermal stability of glasses decrease with increase in B_2O_3 substitution by Al_2O_3. In general Al_2O_3 improves thermal stability of seal glass by hindering phase separation when Al^{3+} ions are 4-coordinated. However, in 6-coordinated state it acts

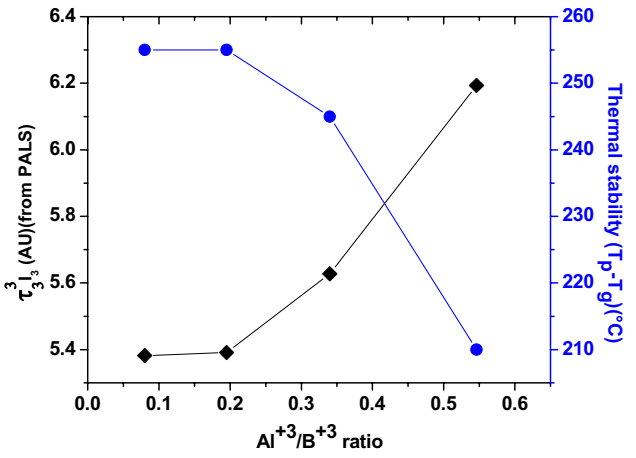

Fig. 8 Thermal stability of glasses against Al^{3+}/B^{3+} ratios in the glasses

as a modifier and enhances phase separation [38]. In the investigated glasses as shown in Fig. 6, a decreasing thermal stability with increasing substitution of B_2O_3 by Al_2O_3 may be attributed to the increasing free volume which thermodynamically favours the crystallization kinetics.

5 Conclusions

In summary, we posit that PALS is a useful technique to probe the subnanoscopic free volume of multinuclear oxide glasses and establish trend-based structure–property correlations. In the investigated series of glasses we have found that the Al^{3+}/B^{3+} ratios dependence of a host of thermo-physical properties could be rationalized in terms of a singular free volume parameter $\tau_3^3 I_3$. This single parameter accurately captures the changes in glass transition temperature, glass softening temperature, coefficient thermal expansion, thermal stability, molar volume and the compactness of the glass systems as a function of progressive substitution of B_2O_3 by Al_2O_3. This indicates that the free volume can be universally applied in the prediction of macroscopic properties of network glasses. Moreover, the approach can be applied to understand the microstructural origins of glass properties. Thereby, the approach can also be applied to design glasses with optimized properties based on their composition including sealants for SOFC applications.

Funding The experimental study under this reported work was not funded by any agency and the investigation was carried out by all authors solely on their own scientific interest.

Compliance with Ethical Standards

Conflict of interest The authors declare that they have no conflict of interest on this reported work.

References

1. N. Ollier, T. Charpentier, B. Boizot, G. Petite, A structural approach by MAS NMR spectroscopy of mechanisms occurring under β-irradiation in mixed alkali aluminoborosilicate glasses. J. Phys. **16**, 7625–7636 (2004)
2. F. Angeli, T. Charpentier, S. Gin, J.C. Petit, ^{17}O 3Q-MAS NMR characterization of a sodium aluminoborosilicate glass and its alteration gel. Chem. Phys. Lett. **341**, 23–28 (2001)
3. J.M. Egan, K.T. Mueller, Detection and identification of corrosion products of sodium aluminoborosilicate glasses by ^{23}Na MQMAS and $^{1}H \rightarrow {}^{23}Na$ CPMAS NMR. J. Phys. Chem. B **104**, 9580–9586 (2000)
4. M.K. Mahapatra, K. Lu, Glass based seals for solid oxide fuel and electrolyzer cells-a review. Mater. Sci. Eng. R **67**, 65–85 (2010)
5. R.K. Brow, D.R. Tallant, Structural design of sealing glasses. J. Non-Cryst. Solids **222**, 396–406 (1997)
6. R.K. Brow, R.D. Watkins, (1991) *High Expansion Li Corrosion Resistant Sealing Glasses*, US Patent 5021307
7. A.J. Cramer, J.M. Cole, V. FitzGerald, M.A. Roberts, T. Brennan, R.A. Martin, G.A. Saunders, R.J. Newport, Effects of rare-earth co-doping on the local structure of rare-earth phosphate glasses using high and low energy X-ray diffraction.. Phys. Chem. Chem. Phys. **15**, 8529–8543 (2013)
8. M. Fábián, E. Sváb, G. Mészáros, L. Kőszegi, L. Temleitner, E. Veress, Neutron diffraction structure study of borosilicate based matrix glasses. Z. Kristallogr. **23**, 461–466 (2006)
9. G.S. Henderson, G. Calas, J.F. Stebbins, The structure of silicate glasses and melts. Elements **2**, 269–273 (2006)
10. A. Zeidler, K. Wezka, R.F. Rowland, DAJ Whittaker, P.S. Salmon, A. Polidori, JWE Drewitt, S. Klotz et.al., High-pressure transformation of SiO_2 glass from a tetrahedral to an octahedral network: a joint approach using neutron diffraction and molecular dynamics. Phys. Rev. Lett. **113**(13), 135501 (2014)
11. M. Reben, E. Golis, J. Filipecki, M. Sitarz, K. Kotynia, P. Jelen, I. Grelowska, Voids in mixed-cation silicate glasses: studies by positron annihilation lifetime and Fourier transform infrared spectroscopies. Spectrochim. Acta. Part A **129**, 643–648 (2014)
12. T. Furukawa, K.E. Fox, W.B. White, Raman spectroscopic investigation of the structure of silicate glasses. III. Raman intensities and structural units in sodium silicate glasses. J. Chem. Phys. **75**, 3226–3227 (1981)
13. T. Furukawa, W.B. White, Raman spectroscopic investigation of sodium borosilicate glass structure. J. Mater. Sci. **16**, 2689–2700 (1981)
14. M.N. Garaga, M.-F. Hsieh, Z. Nour, M. Deschamps, D. Massiot, B.F. Chmelka, S. Cadars, Local environments of boron heteroatoms in non-crystalline layered borosilicates. Phys. Chem. Chem. Phys. **17**, 21664–21682 (2015)
15. B. Pahari, S. Iftekhar, A. Jaworski, K. Okhotnikov, K. Jansson, B. Stevensson, J. Grins, M. Edén, Composition-property-structure correlations of scandium aluminosilicate glasses revealed by multinuclear ^{45}Sc, ^{27}Al and ^{29}Si solid state NMR. J. Am. Ceram. Soc. **95**(8), 2545–2553 (2012)
16. G. Brown, G. Waychunas Jr., C. Ponader, W. Jackson, D. Mckeown, EXAFS and NEXAFS studies of cation environments in oxide glasses. J. Phys. Colloq. **47**(C8), 661–668 (1986)
17. R. Golovchak, A. Ingram, S. Kozyukhin, O. Shpotyuk, Free volume fragmentation in glassy chalcogenides during natural physical ageing as probed by PAL spectroscopy. J. Non-Cryst. Solids **377**, 49–53 (2013)
18. M.D. Ingram, S.J. Pas, C. Cramer, Y. Gao, A.J. Hill, Free volume anomalies in mixed cation glasses revealed by positron annihilation lifetime spectroscopy (PALS). Phys. Chem. Chem. Phys. **7**, 1620–1623 (2005)

19. P.K. Ojha, S.K. Rath, S.K. Sharma, K. Sudarshan, P.K. Pujari, T.K. Chongdar, N.M. Gokhale, Free volume of mixed cation borosilicate glass sealants elucidated by positron annihilation lifetime spectroscopy and its correlation with glass properties. J. Power Sources **273**, 937–944 (2015)
20. A. Feltz, *Amorphous and Vitreous Inorganic Solids* (Mir, Moscow, 1986), p. 556
21. M. Kastner, Compositional trends in the optical properties of amorphous lone-pair semiconductors. Phys. Rev. B **7**, 5237–5252 (1973)
22. O. Shpotyuk, J. Filipecki, *Free Volume in Vitreous Chalcogenide Semiconductors: Possibilities of Positron Annihilation Lifetime Study* (WSP, Czestochowa, 2003), p. 114
23. D.S. Sanditov, S. S. Sangadiev, A new approach to the interpretation of fluctuation free volume of amorphous polymers and glasses. Sov. Vysokomol. Veshchestva **41**, 1–24 (1999)
24. R. Zallen, *The Physics of Amorphous Solids* (Wiley, Hoboken, 1983), p. 192
25. S.A. Dembovsky, E.A. Chechetkina, *Glass-formation* (Nauka, Moscow, 1990), p. 279
26. K. Sudarashan, S.K. Rath, M. Patri, P.K. Pujari, Positron annihilation spectroscopic studies of fluorinated ethylene propylene copolymer-*g*-polystyrene. Polymer **48**, 6434–6438 (2007)
27. P.N. Patil, S.K. Rath, S.K. Sharma, K. Sudarshan, P. Maheshwari, M. Patri, S. Praveen, P. Khandelwal, P.K. Pujari, Free volumes and structural relaxations in diglycidyl ether of bisphenol-A based epoxy-polyether amine networks. Soft Matter **9**, 3589–3599 (2013)
28. S.K. Sharma, J. Prakash, J. Bahadur, K. Sudarshan, P. Maheswari, S. Mazumdar, P.K. Pujari, Investigation of nanolevel molecular packing and its role in thermo-mechanical properties of PVA-fMWCNT composites: positron annihilation and small angle X-ray scattering studies. Phys. Chem. Chem. Phys. **16**, 1399–1408 (2014)
29. S.K. Rath, K. Sudarshan, R.S. Bhavsar, U.K. Kharul, P.K. Pujari, M. Patri, D.V. Khakhar, Characterizing the nanoclay induced constrained amorphous region in model segmented polyurethane-urea/clay nano composites and its implications on gas barrier properties. Phys. Chem. Chem. Phys. **18**(3), 1487–1499 (2016)
30. M. Zanatta, G. Baldi, R.S. Brusa, W. Egger, A. Fontana, E. Gilioli, S. Mariazzi, G. Monaco et.al., Structural evolution and medium range order in permanently densified vitreous SiO_2. Phys. Rev. Lett. **112**, 045501 (2014)
31. K.S. Weil, The state of the art in sealing technology for solid oxide fuel cells. J. Miner. Met. Mater. Soc. **58**, 37–44 (2006)
32. V.A.C Haanappel, V. Shemet, S.M. Gross, T. Koppitz, N.H. Menzler, M. Zahid, W.J. Quadakkers, Behaviour of various glass–ceramic sealants with ferritic steels under simulated SOFC stack conditions. J. Power Sources **150**, 86–100 (2005)
33. K.D. Meinhardt, D.-S. Kim, Y.-S. Chou, K.S. Weil, Synthesis and properties of a barium aluminosilicate solid oxide fuel cell glass–ceramic sealant. J. Power Sources **182**, 188–196 (2008)
34. P. Kirkgraad, N.J. Pedersen, M. Eldrup, PATFIT (RISO National Laboratory, Denmark, 1998)
35. K. Inoue, H. Kataoka, Y. Nagai, M. Hasegawa, Y. Kobayashi, Short and medium range order in two-component silica glasses by positron annihilation spectroscopy. J. Appl. Phys. **115**, 204903 (2014)
36. M. Eldrup, D. Lightbody, J.N. Sherwood, The temperature dependence of positron lifetimes in solid pivalic acid. Chem. Phys. **63**, 51–58 (1981)
37. L. Tichy, H. Ticha, On the chemical threshold in chalcogenide glasses. Mater. Lett. **21**, 313–319 (1994)
38. J.E. Shelby, *Introduction to glass science and technology*, 2nd edn. (The Royal society of Chemistry, Cambridge, 2005)
39. M.B. Volf, *Chemical Approach to Glass. Glass Science and Technology*. (Elsevier, New York, 1984)
40. H. Scholze, *Glass Nature, Structure, and Properties*. (Springer Verlag, New York, 1991)
41. G. Saffarini, J. Matthiesen, R. Blachnik, The influence of mechanical and chemical thresholds on the free volume percentage in Ge–Se–(Fe, In) chalcogenide glasses. Phys. B **305**, 293–297 (2001)
42. R.N. Singh, Sealing technology for solid oxide fuel cells (SOFC). Int. J. Appl. Ceram. Technol. **4**, 134–144 (2007)
43. H.D. Ackler, Healing of lithographically introduced cracks in glass and glass containing ceramics. J. Am. Ceram. Soc. **81**, 3093–3103 (1998)
44. P. Hrma, W.T. Han, A.R. Cooper, Thermal healing of cracks in glass. J. Non Cryst. Solids **102**, 88–94 (1988)